RSC Advances

ROYAL SOCIETY OF CHEMISTRY

www.rsc.org/advances

Safranin and cysteine capped gold nanoparticles, spectroscopic qualitative and quantitative studies

F.Aghajanloo[1], S. Nouroozi[1*], K. Rostamizadeh[2]

[1]Department of Chemistry, University of Zanjan, 45371-38791, Zanjan, Iran

[2]Zanjan pharmaceutical nanotechnology research center, Zanjan University of Medical Science, Zanjan, Iran

Keywords: Gold nanoparticles; Safranin; Cysteine; Spectrofluorimetry; Spectrophotometry; Light Scattering.

Abstract

The interaction between cysteine and safranin with citrate capped gold nanoparticles was studied. All measurements were carried out using resonance light scattering (RLS), UV–Vis. absorption and fluorescence spectrometry. The size and surface characteristics of safranin-capped gold nanoparticles in the solution containing cysteine was also investigated by dynamic light scattering (DLS) and transmission electron microscopy (TEM) techniques. The average diameter and surface potential of synthesized GNPs were 19.0 nm and -56.3 mV, respectively. Interaction of the GNPs and safranin or cysteine leads to increase their sizes and surface potentials. The influence of parameters such as pH, ionic strength of the solution and safranin concentration was studied on the spectrophotometric and spectrofluorimetric characteristics of GNPs. This system was used for determining cysteine content of unknown solutions. In the optimum conditions (pH, 4; sodium chloride, 0.014 M and safranin, 9.0×10^{-6} M) two linear dynamic ranges (9.0×10^{-8}–1.0×10^{-6} M and 5.0×10^{-6}–9.0×10^{-5} M) with RSD less than 5% was obtained for cysteine. Limit of detection under the optimized conditions was 3.7×10^{-8} M of cysteine. Kinetic studies of safranin and cysteine adsorption on the surface of GNPs were carried out and their corresponding rate constants were also calculated using kinetic models.

* Corresponding author: s.nouroozi@znu.ac.ir, Tel: +98 24 3305 2590, Fax: +98 24 3305 2477.

1. Introduction

Gold nanoparticles (GNPs) because of their unique physical and chemical properties are considered as an important class of nanomaterials that gain worldwide attention in recent years. GNPs are preferred candidate in the fabrication of smart sensing devices for detection of special biomolecules such as amino acids, various forms of proteins and DNA [1]. GNPs offer several benefits in sensory researches [2]. They have excellent compatibility with almost all types of chemically (organic and metallic) and biologically active molecules. This property is important because the functional activity of these molecules unaffected even after their immobilization on the nanoparticles. Moreover, GNPs have high surface area to volume ratios, so they can be served as an excellent scaffold to immobilize large quantities of organic and/or biomolecules, which leads to increase of their interactions with target analytes. Citrate capped GNPs are negatively charged; so they can electrostatically interact with certain positively charged proteins, which results in specific interaction with the target analyte of interest. Furthermore, GNPs can be monitored by various detection methods (spectrophotometric, spectrofluorimetric and electrochemical methods), so an analyte can be sensed through more than one detection mode.

Recently, surface plasmon resonance (SPR) analysis technique has gained more attention particularly in biological and biochemical studies. SPR signal frequencies for metal nanoparticles depend on the shape, size and dielectric properties of nanoparticles medium. GNPs with particle sizes between 15 nm to 150 nm show special signal frequencies (i.e. red color) in SPR [3–5]. Resonance light scattering (RLS) is the other technique, which has been used to study GNPs [6, 7]. Scattering of the light by GNPs with diameters less than 1/20 wavelength of incident light could be monitored using a spectrofluorimeter. The RLS effects are observed at or very near to the wavelength of absorption of an aggregated species. These effects can be dramatically enhanced when strong electronic coupling exists among the chromophores. GNPs are red in color because of the absorption by their surface plasmon oscillation at 520 nm, so, the light scattering peak of GNPs at 520 nm can be characterized as the RLS peak [8–11]. In recent years, techniques based on measuring resonant light scattering signals of GNPs for measurements of proteins, DNA, glucose and amino thiol compounds are increasingly used in pharmaceutical studies [12–15]. The high sensitivity and low response times are special characteristics of all these methods.

Cysteine is one of the important sulfur containing amino acid in living systems [16]. Determination of cysteine and its metabolite in urine is useful in the diagnosis of human diseases such as cystinuria and also in drug therapy monitoring [17–19]. Currently, determination of cysteine

is carried out using various techniques, including optical spectroscopy [20–22], electrochemical methods [23], flow injection analysis [24, 25], high-performance liquid chromatography or gas chromatography with fluorescence, absorbance or mass spectrometry detection [26–28]. Drawbacks such as the cross-reactivity with other amino acids and the required cumbersome laboratory procedures, limit extensive clinical applications for many of these methods. There are also several reports in the literature in which RLS response has been used for determination of cysteine and other thiol containing amino acids [7, 16, 29, and 30]. Although these methods offer high sensitivity and low detection limits but they have disadvantages such as time consuming, poor selectivity and cumbersome laboratory procedure. In the present work, the spectrophotometric, spectrofluorimetric and RLS characteristics of GNPs are studied in the presence of safranin and cysteine, simultaneously. The method has also been used for cysteine determination.

2. Experimental

2.1 Reagents and chemical materials

Gold (III) chloride trihydrate ($HAuCl_4 \bullet 3H_2O$) and sodium citrate (Merck) were used for the synthesis of gold nanoparticles. Safranin (Fluka) and sulfur containing amino acids (Merck) were used to prepare standard solutions using deionized water. Britton-Robinson buffer was used for adjusting the pH of all solutions.

2.2 Apparatus

UV–Vis spectrophotometer (Thermo, model GENESYS 10uv) and spectrofluorometer (HITACHI, F-2500) were used for absorption and RLS measurements, respectively. Emission spectrums were recorded from 400 nm to 700 nm by the excitation of the solutions at 520 nm and 490 nm through a quartz cell with a path length of 1cm. Transmission electron microscopy, TEM (EM 208- Philips) was used for particles size measurements. Dynamic light scattering, DLS (Zetasizer instrument Nano–ZS, MALVERN) was also used to study the particle size and surface potential. Metrohm pH meter (827 pH lab) was used to measure pH of the solutions. All measurements were carried out at 25.0±0.1°C.

2.3 General procedures

Synthesis of gold nanoparticles

Gold nanoparticles were prepared by reducing $HAuCl_4$ in the presence of sodium citrate (Turkevich technique) [31, 32]. To prevent nanoparticles from agglomeration during the synthesis, all glassware were washed with HCl: HNO_3 (3:1) solution, then with distilled water and oven-dried. In summary, 50 mL of 1 mM $HAuCl_4$ solution was heated under reflux to the boiling point. Then 5 mL of 38.8 mM of sodium citrate was added to the solution which continuously stirring and boiling for half an hour. After completion of Au^{3+} ion reduction the prepared solution was cooled at room temperature and stored in the refrigerator (4°C) for later uses.

Preparation of GNPs coated with safranin and cysteine

Aliquots volumes of GNPs, safranin and cysteine solutions were mixed in 2.5 mL vials and after addition of sodium chloride (14.0 mM) and Britton-Robinson buffer (0.4.m M, pH 3–7) for ionic strength and pH adjusting, resulted solution was diluted by DI water. All cysteine and other amino acid solutions were prepared freshly.

3. Results and discussions

3.1. Characterization of synthesized gold nanoparticles

TEM images of synthesized GNPs and distribution of their diameters are shown in Fig. 1A and 1B, respectively. DLS data for the bared and capped GNPs are shown in the table 1 and Figures S1–S3. The average diameter and surface potential of synthesized nanoparticles were obtained to be ~19.5 nm and -56.3 mV, respectively.

Fig. 1A and 1B positioned here.

According to Cortie and Van der Lingen [32] the concentration of synthesized nanoparticles can be calculated using the following equation:

$$(\frac{d_{AuNP}}{2})^3 \approx nr_{Au}^3 \times \frac{1}{0.7} \rightarrow d_{AuNP}^3 \approx 0.0342n$$

In this equation, d is diameter of nanoparticle; n is the number of gold atoms with radius of r and 70 percent cumulative density. Concentration of the synthesized GNPs in the solution was calculated to be 5.0 nM at pH 5.5.

Table 1 positioned here.

3.2 Study on behavior of GNPs coated with safranin

According to the DLS results (table 1 and Fig. S2), by addition of safranin to the GNPs solution, the surface potential of particles would be positive (i.e. 5.22 mV) and leads to a larger particle size (i.e. 657.5 nm) due to the electrostatic interaction between the negative carboxylate groups on the surface of gold nanoparticles and safranin molecules. Consequently, the red gold nanoparticles would be aggregated and converted to a blue solution. RLS and Visible spectrums of GNPs coated safranin (Fig. 2A and 2B) confirmed these results. The intensity of maximum absorption of GNPs coated with safranin at 530 nm is increased, their RLS peak at 520 nm is reduced sharply and the fluorescence of safranin molecules quenches as a results of these interactions. Complex of gold nanoparticles–safranin is a combination structure consists of three layers of gold nanoparticles as the core and citrate as a bridge for binding of safranin molecules [1].

Fig. 2A and 2B positioned here.

Effects of ionic strength

Ionic strength of the solution has special effect on the behavior of solution particles. Variations of the RLS intensity of GNPs coated safranin as a function of ionic strength of the solution (NaCl concentration) are shown in Fig. 3. Electrolyte has critical effect in accumulation process due to squeezing the electric double layer [33, 34]. The obtained experimental data revealed that higher ionic strength accelerates the nanoparticles accumulation process and then RLS intensity reaches to a maximum at NaCl concentration of 14.0 mM. In the electrolyte concentrations more than 14.0 mM, RLS intensity decreases because of destruction electrostatic interaction between ammonium (in the safranin molecule) and carboxylate (on the surface of GNPs). 14.0 mM of NaCl was chosen as optimal electrolyte concentration.

Fig. 3 positioned here.

Effects of the solution pH

The pH of GNPs and GNPs containing safranin solutions in the optimum electrolyte concentration were changed from 3 to 7. Results of RLS studies are shown in Fig. 4. Optimum pH of 4 was obtained for both of the solutions. High acidic medium, leads to protonation of carboxylate groups of citrate on the GNPs and then the aggregation of nanoparticles take place. In the pH range of 3.5–4.5, all of the safranin species are in the monomer (R^+) forms and strong electrostatic

interaction between $-NH_3^+$ groups on the safranin molecules and $-COO^-$ groups in the surface of GNPs leads to enhanced RLS signals. At higher pH, deprotonation of the safranin molecules leads to destruction of electrostatic interaction and then reducing of RLS intensities.

Fig. 4 positioned here.

Effects of the safranin concentration

The effects of safranin concentration on the behavior of GNPs solutions were studied and the results are shown in Figures 5 and 6. Increasing safranin concentration in the GNPs solution, leads to increase in the intensity of absorption of GNPs at 530 nm. Only in the low concentrations of safranin, the intensity of this absorption peak was reduced and a wide peak at 700 nm was obtained. According to the results in Fig. 6A and 6B, RLS intensity of GNPs decreases with increasing the safranin concentration and the fluorescence intensity of safranin solution at λ_{em} 580 nm was increased up to 3×10^{-5} M and then decreased. However, at concentrations below 3×10^{-5} M of safranin, the predominant forms of safranin are cationic monomers that attract electrostatically to the negatively charged carboxylate ion on the GNPs, whereas at the higher concentration, safranin forms dimmers $(R_2)^{2+}$, which binds to the nanoparticles loosely [1]. Formation of binary or ternary species of safranin molecules leads to a blue shift of the absorption spectrum and fluorescence quenching of safranin solution. At high concentrations of safranin, however, the self accumulation between safranin species competes with the formation of nanoparticles–safranin complex. Therefore safranin concentration should be less than 3×10^{-5} M in all solutions.

Fig. 5 and 6 positioned here.

3.3 Study on the behavior of GNPs coated with safranin in the presence of cysteine

DLS data of solution containing GNPs–safranin complex and cysteine are shown in table 1 and Fig. S3. According to these results, by addition of cysteine, the surface charges of nanoparticles become more positive (6.74 mV) and particles sizes are also very large (1484 nm). RLS spectrum of this system is shown in Fig. 7.

Fig. 7 positioned here.

The effect of cysteine on the visible spectrum is not so clear but on the light scattering spectrum it causes a decrease in the intensity at 520 nm. Actually, by addition of cysteine to the solution, the –SH group of cysteine will form Au–S covalent bond and $-NH_2$ group will also form

electrostatic binding to the negatively charged surface of gold nanoparticles which leads to form a network structure in the surface of GNPs [7, 35]. This characteristic of interaction of cysteine with safranin coated GNPs have important role in the sensory behavior of the system in the cysteine determination.

Effects of ionic strength and pH

According to the results in the Fig. 8 and 9, the effects of ionic strength and pH on the behavior of GNPs–safranin–cysteine are the same as the GNPs–safranin system, which discussed earlier in this article. Maximum RLS intensity for GNPs–safranin–cysteine system is also at pH 4 and NaCl of 14.0 mM. Since, the pK_a value of the $–NH_3^+$ group of cysteine is about 10.8, in the pH of 4, cysteine is positively charged. On the other hand, the ionization of –COOH groups in the citrate ion is increased up to pH 4. Consequently, increasing electrostatic interactions of the $–COO^-$ and the $–NH_3^+$ groups leads to increase of RLS intensity.

Fig. 8 and 9 positioned here.

3.4 Measurement of cysteine by the GNPs–safranin system

GNPs–safranin system was used for quantifying cysteine content in a solution. To obtain a calibration curve for cysteine, to a 1 ml solution of nanoparticles with sodium chloride of 14.0 mM (to adjust the ionic strength), Britton–Robinson buffer of pH 4 and in the presence of 9.0×10^{-6} M of safranin, various volumes of cysteine was added and RLS peak intensity at λ_{ex} 520 nm as analytical signals were recorded. According to the results, two linear dynamic in the ranges of 9.0×10^{-8} – 1.0×10^{-6} M and 5.0×10^{-6} – 9.0×10^{-5} M with good correlation coefficient (r^2=0.99) were obtained for cysteine determination. RSD (n=3) for these measurements was less than 5 % and detection limit of 3.7×10^{-8} M cysteine was also obtained. Table 2 summarized analytical results in the cysteine determination for proposed method and many other methods [7, 16, 29 and 30] which are showing the priority of proposed method over many of these techniques.

Table 2 positioned here.

3.5 Kinetic studies of safranin adsorption and rates of thiol displacement

Figure 10 represents the time evolution of light scattering quenching by GNPs–safranin system in which quenching reaches to its minimum value after 80 minutes. Adsorption of safranin onto the GNPs is very fast and the light scattering quenching follows an exponential decay curve as:

$F(t) = A_1\exp(-K_1 t) + A_2\exp(-K_2 t)$. Fitting of experimental data to this equation provides safranin adsorption rate constants as $K_1 = 2.60\times10^{-2}$ s^{-1}, $K_2 = 1\times10^{-4}$ s^{-1}, $A_1 = 0.99$ and $A_2 = 0.06$. Displacement of citrate on the GNPs by safranin is considered to be the faster kinetic step. With increasing GNPs surface coverage as a result of adsorption of more safranin molecules, the adsorption rate should be decreased because of steric effects between the safranin molecules on the GNPs surface, so K_2 is the rate constant for slower reaction. Addition of cysteine to the safranin coated GNPs leads to increase in the fluorescence intensity of the safranin at λ_{em}= 580 nm as a result of desorption of the safranin from the GNPs and displacement of it by cysteine. Figure 11 indicates this phenomenon, in which the fluorescence intensity at 580 nm increasing gradually. These experimental data show a good fitting with the following bi-exponential equation: $F(t) = K'_1(1-\exp(-K_{obs1} t)) + K'_2(1-\exp(-K_{obs2} t))$, in which $K_{obs} = K_a C + K_d$ and K_a and K_d are adsorption and desorption constants, respectively. Fitting of experimental results in the figure 11 give us the following data: $K'_1 = 0.965$ s^{-1}, $K_{obs1} = 3.82$ s^{-1}, $K'_2 = 0.574$ s^{-1} and $K_{obs2} = 2.2\times10^{-2}$ s^{-1}. Desorption rates of the thiol are much lower than their adsorption rates because of their strong Au–S interaction ($K_d << K_a$), so we can ignore the term K_d and thus at a constant thiol concentration, K_{obs} can be reflected as the magnitude of K_a.

Fig. 10 and 11 positioned here.

Conclusion

In the present work, the spectroscopic (spectrophotometric, spectrofluorimetric and RLS) characteristics of gold nanoparticles in the presence of safranin and cysteine were studied. The measurements performed using resonance light scattering and absorption spectroscopy. The size and surface characteristics of safranin-coated gold nanoparticles in the solution containing cysteine were also investigated by DLS and TEM techniques. Average diameter of the synthesized Au nanoparticles was about 19.5 nm and their surface potential was -56.3 mV. The ionic strength of the solution is critical in self accumulation process for GNPs; therefore, NaCl concentration should be kept lower than 20.0 mM. The effects of ionic strength and pH on the GNPs–safranin–cysteine system are similar to the GNPs–safranin system. Maximum RLS intensities were obtained at pH 4 and 14.0 mM of NaCl concentration. This system was also used for measuring cysteine content of a solution. Using RLS peak intensity at 520 nm as analytical signal and in the optimum conditions, two linear ranges for cysteine determination were obtained in the ranges 9×10^{-8} to 1×10^{-6} M and 5×10^{-6} to 9×10^{-5} M with RSD < 5%. Limit of detection in the optimum conditions was also obtained

as 3.7×10^{-8} M of cysteine. Kinetic studies of interactions between GNPs, safranin and cysteine were carried out and related rate constants were calculated using data of kinetic studies.

Acknowledgements

The research presented in this paper was supported by the University of Zanjan research programs of Higher Education. The authors also are gratefully acknowledged to the Zanjan University of Medical Science for supporting of this work.

References:

[1] H. Youqiu, L. Shaopu, L. Qin, L. Zhongfang & H. Xiaoli, *Sci. China, Ser. B.,* 2005, **48,** 216.

[2] V.K.K. Upadhyayula, *Anal. Chim. Acta,*2012, **715**, 1.

[3] D. B. Pedersen, E.J.S. Duncan, *Technical Report DRDC Suffield TR*, 2005, **109**.

[4] C. Burns, W.U. Spendel, S. Puckett, G.E., *Talanta,* 2006, **69,** 873.

[5] C. Z. Huang, Y. F. Li, *Anal. Chim. Acta,* 2003, **500,** 105.

[6] W.Z. Yang, *Physical Chemistry Techniques,* Peking University Press, Beijing, 1992.

[7] Z. P. Li, X. R. Duan, C. H. Liu, B. A. Du, *Anal. Biochem.* 2006, **351**, 18.

[8] R.F. Pasternack, P.J. Collings, *Science,* 1995, **269**, 935.

[9] K.C. Grabar, R.G. Freeman, M.B. Hommer, M.J. Natan, *Anal. Chem*. 1995, **67**, 735.

[10] U. Kreibig, L. Genzel, *Surf. Sci.* 1985, **156**, 678.

[11] H. S. Jung, J. H. Han, T. Pradhan, S. Kim, S. W. *Biomaterials* 2012, **33**, 945.

[12] L. Shang, J. Yin, J. Li, L. Jin, S. Dong, *Biosens. Bioelectron.* 2009, **25**, 269.

[13] Q. Xiao, F. Shang, X. Xu, Q. Li, C. Lu, *Biosens. Bioelectron,* 2011, **30**, 211.

[14] J. Ezzati Nazhad Dolatabadi, O. Mashinchian, B. Ayoubi, A. A. Jamali, A. Mobed, D. Losic, Y. Omidi, *Trends Anal. Chem.* 2011, **30**, 459.

[15] J., Turkevich, P.C., Stevenson, and J., Hillier, *Discuss. Faraday Soc.*, 1951, **11**, 55.

[16] Q. Xiao, L Zhang, Ch. Lu, *Sens. Actuators B*, 2012, **166– 167**, 650.

[17] E. Kaniowska, G. Chwatko, R. Glowacki, P. Kubalczyk, E. Bald, *J. Chromatogr. A,*1998, **798**, 27.

[18] Y.Q. Huang, G.D. Ruan, J.Q. Liu, Q. Gao, Y.Q. Feng, *Anal. Biochem.* 2011, **416**,159.

[19] K. Kusmierek, R. Glowacki, E. Bald, *Anal. Bioanal. Chem.* 2006, **385,** 855.

[20] M.J. Li, C.Q. Zhan, M.J. Nie, G.N. Chen, X. Chen, *J. Inorg. Biochem.* 2011, **105,** 420.

[21] O. Rusin, N.N.S. Luce, R.A. Agbaria, J.O. Esconedo, S. Jiang, I.M. Warner, F.B.

Dawan, K. Lian, *J. Am. Chem. Soc.*2004, **126**, 438.

[22] Q.Q. Li, F. Shang, C. Lu, Z.X. Zheng, J.M. Lin, *J. Chromatogr. A*, 2011, **1218**, 9064.

[23] W.R. Jin, Y. Wang, *J. Chromatogr. A*, 1997, **769**, 307.

[24] Ali A. Ensafi, B. Rezaei, and S. Nouroozi, *J. Braz. Chem. Soc.*, 2009, **20**, 288.

[25] B. Rezaei, Ali A. Ensafi, S. Nouroozi, *Anal. Sci.*, 2005, **21**, 1067.

[26] G. Cevasco, A.M. Piatek, C. Scapolla, S. Thea, *J. Chromatogr. A*, 2010, **1217**,2158.

[27] C. Hellmuth, B. Koletzko, W. Peissner, *J. Chromatogr. B,* 2011, **879**, 83.

[28] R. Glowacki, E. Bald, *J. Chromatogr. B*, 2009, **877**, 3400.

[29] J. Wanga, Y. F. Li, Ch. Z. Huanga, T. Wua, *Anal. Chim. Acta,* 2008, **626**, 37.

[30] H. Tavallali, A. Amouri*, Int. J. ChemTech Res.*, 2012, **4,** 297.

[19] A. Mocanua, I. Cernicab, G. Tomoaiac, L. D. Bobosa, O. Horovitz, M. Tomoaia-Cotisel, *Colloids Surf. A.,* 2009, **338**, 93.

[31] J., Kimling, M., Maier, B., Okenve, V., Kotaidis, H., Ballot, and A., Plech, *J. Phys. Chem. B*, 2006, **110**, 15700.

[32] M.B. Cortie and E.V.D. Lingen, *Mater. Forum,* 2002, **26,** 1.

[33] A. Santosh, K.C. Remant Bahadur, N. Bhattarai, K. K. Chul, Y. K. Hak, *J. Colloid Interface. Sci.,* 2006, **299**, 191.

[34] M.R. Hormozi-Nezhad, E. Seyedhosseini, H. Robatjazi, *Sci. Iran.,* 2012, **19,** 958.

[35] K.H. Lee, S. J Chen, J. Y. Jeng, Y. C. Cheng, J. T. Shiea, H.T. Chang, *J. Colloid Interface. Sci.*, 2007, **307**, 340.

Supplementary Figures:

Fig. S1, S2 and S3 positioned here.

Figures captions:

Fig.1. A: TEM images and B: particles size distribution of synthesized GNPs (5 nM).

Fig.2. RLS (A) and visible spectrum (B) for GNPs, safranin and GNPs coated safranin. Conditions: GNPs, 2.0 nM; safranin, 50.0 μM; Briton–Robinson buffer (pH 4.0), 0.4 mM.

Fig.3. Effects of ionic strength of the solutions on the RLS peak intensity for GNPs coated safranin. Conditions: GNPs, 2.0 nM; safranin, 30.0 μM; Briton–Robinson buffer (pH 4.0), 0.4 mM.

Fig.4. Effects of pH of the solutions on the RLS peak intensity for GNPs and GNPs coated safranin. Conditions: GNPs, 2.0 nM; safranin, 30.0 μM; NaCl, 14.0 mM; Briton–Robinson buffer (pH 3.0–6.5), 0.4 mM.

Fig.5. Effects of safranin concentrations on the visible spectrum of the GNPs. Conditions: GNPs, 2.0 nM; NaCl, 14.0 mM; Briton–Robinson buffer (pH 4.0), 0.4 mM.

Fig. 6. A: Variation of RLS peak intensity of GNPs (in the wavelength of 520 nm) as a function of safranin concentrations. B: Variation of fluorescence signal of safranin solution in the emission wavelength of 580 nm. Conditions: GNPs, 2.0 nM; NaCl, 14.0 mM; Briton–Robinson buffer (pH 4.0), 0.4 mM.

Fig.7. RLS spectrum of GNPs coated safranin as a function of different concentration of cysteine. Conditions: GNPs, 2.0 nM; safranin, 9.0 μM; NaCl, 14.0 mM; Briton–Robinson buffer (pH 4.0), 0.4 mM.

Fig.8. Effects of ionic strength on the RLS peak intensity for GNPs–safranin and GNPs–safranin-cysteine solutions. Conditions: GNPs, 2.0 nM; safranin, 9.0 μM; cysteine, 5.0 μM; Briton–Robinson buffer (pH 4.0), 0.4 mM.

Fig.9. Effects of the pH on the RLS peak intensity for GNPs–safranin and GNPs–safranin–cysteine solutions. Conditions: GNPs, 2.0 nM; safranin, 9.0 μM; cysteine, 5.0 μM; NaCl, 14.0 mM; Briton–Robinson buffer (pH 3.0–6.5), 0.4 mM.

Fig.10. RLS peak intensity decay of GNPs in the presence of safranin. The RLS intensities at 520 nm were recorded every 5 min. The concentrations of safranin, GNPs and cysteine were 9μM, 2 nM and 10μM, respectively. NaCl, 14.0 mM; Briton–Robinson buffer (pH 4.0), 0.4 mM.

Fig.11. Fluorescence growth upon replacing the adsorbed safranin molecules on the GNPs–safranin with cysteine. The fluorescence intensities at 580 nm were recorded every 5 min. The concentrations of safranin, GNPs and cysteine were 9μM, 2 nM and 10μM, respectively. NaCl, 14.0 mM; Briton–Robinson buffer (pH 4.0), 0.4 mM.

Supplementary Figures captions:

Fig.S1. DLS results for GNPs (5.0 nM) solutions. A) Intensity percent. B) Zeta potential.

Fig.S2. DLS results for GNPs coated safranin. A) Intensity percent. B) Zeta potential. Conditions: GNPs, 2.0 nM; safranin, 9.0 μM; NaCl, 14.0 mM; Briton-Robinson buffer (pH 4.0), 0.4 mM.

Fig.S3. DLS results for GNPs coated safranin in presence of cysteine. A) Intensity percent. B) Zeta potential. Conditions: GNPs, 2.0 nM; safranin, 9.0 μM; cysteine, 5.0 μM; NaCl, 14.0 mM; Briton-Robinson buffer (pH 3.0-6.5), 0.4 mM.

Table 1: DLS data for nano particles

Particles	Z–Average (d, nm)	Zeta potential (mV)
GNPs	19.58	-56.3
GNPs - Safranin	657.5	5.22
GNPs–Safranin–Cysteine	1484	6.74

Table 2: comparison of analytical data for cysteine determination

Method	Linear Dynamic Range (M)	Detection Limit (M)	RSD (%)	Reference
1	9.0×10^{-8}–1.0×10^{-6} and 5.0×10^{-6}–9.0×10^{-5}	3.7×10^{-8}	< 5	proposed method
2	8.25×10^{-8}–2.06×10^{-6}	1.65×10^{-8}	1.2	[7]
3	8.0×10^{-8}–6.0×10^{-6}	4.0×10^{-8}	–	[16]
4	8.25×10^{-8}–3.3×10^{-6}	2.39×10^{-8}	< 3.6	[29]
5	8.25×10^{-8}–2.55×10^{-6}	4.12×10^{-8}	4.1	[30]

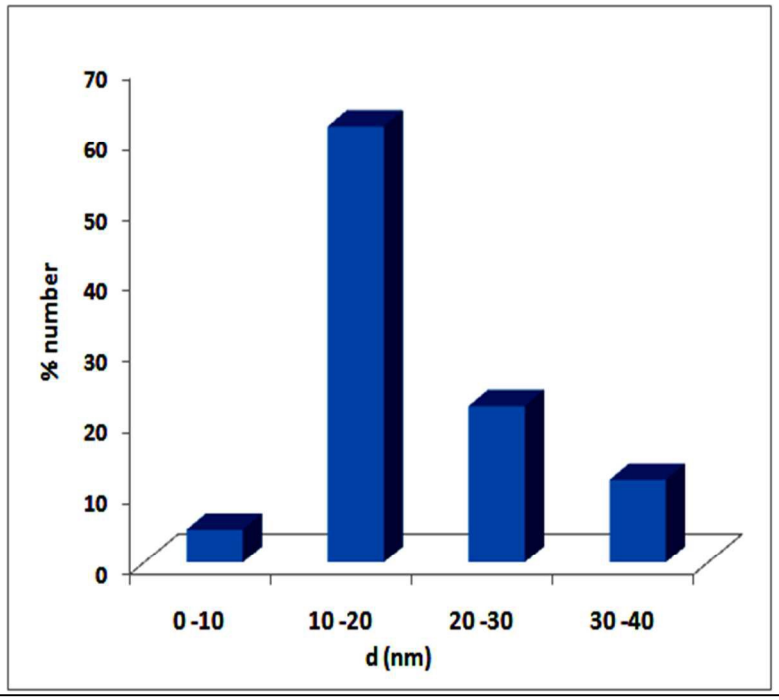

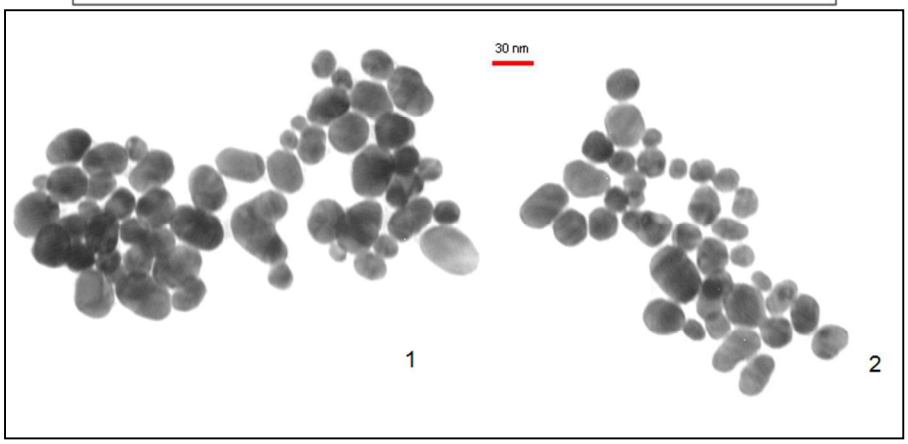

Gold Nanoparticles

Figures:

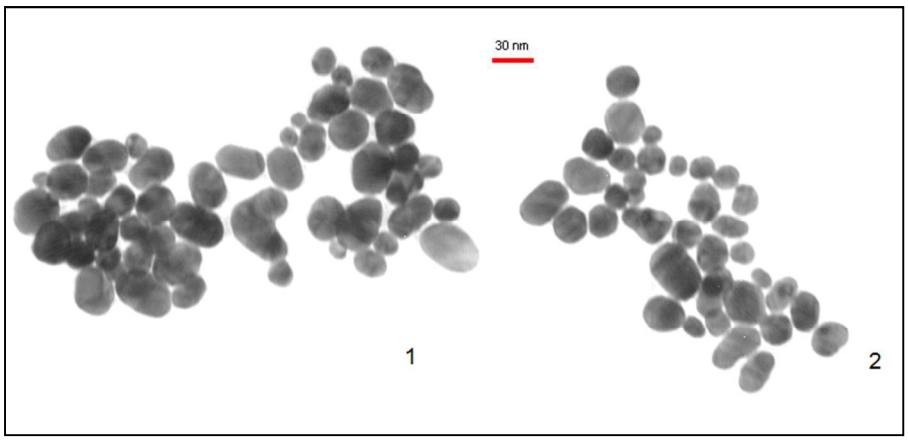

A

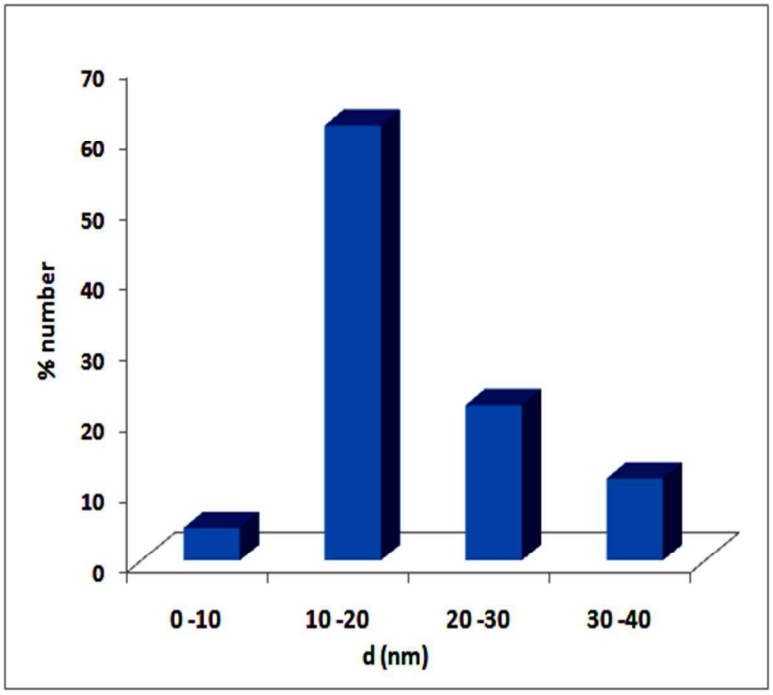

B

Fig. 1

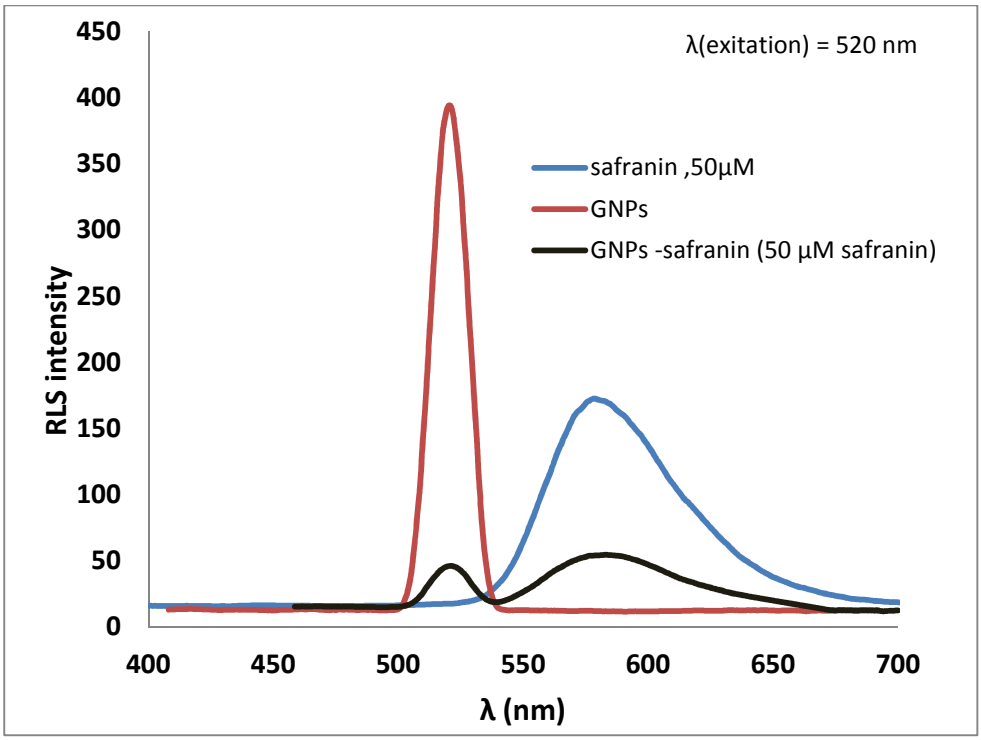

A: RLS spectrum

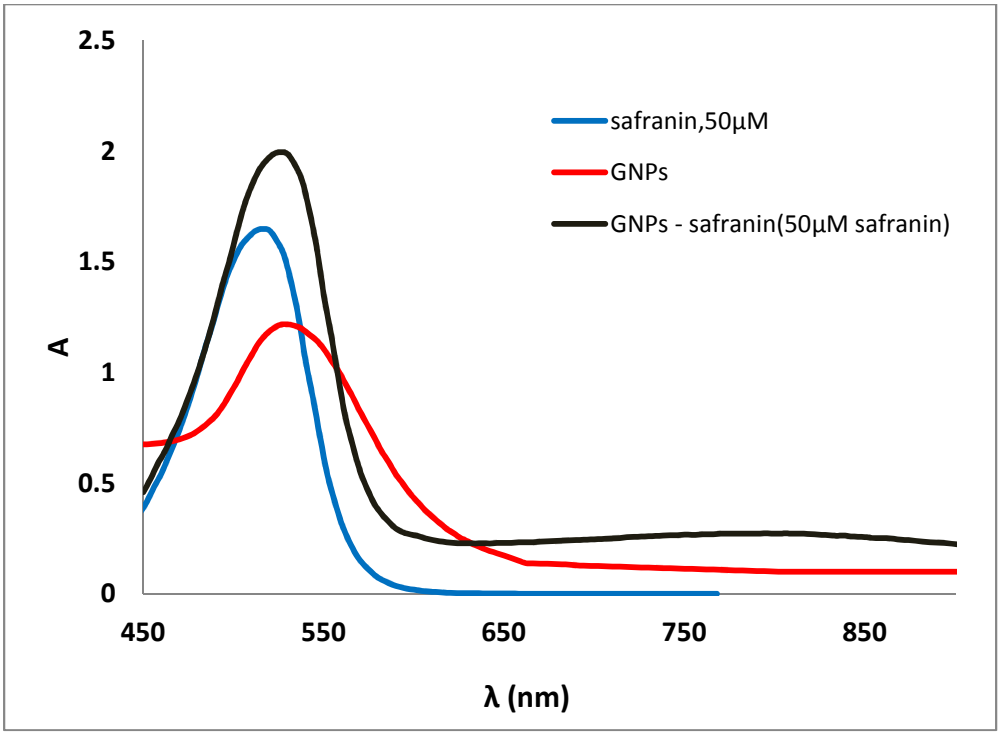

B: visible absorption spectrum

Fig.2

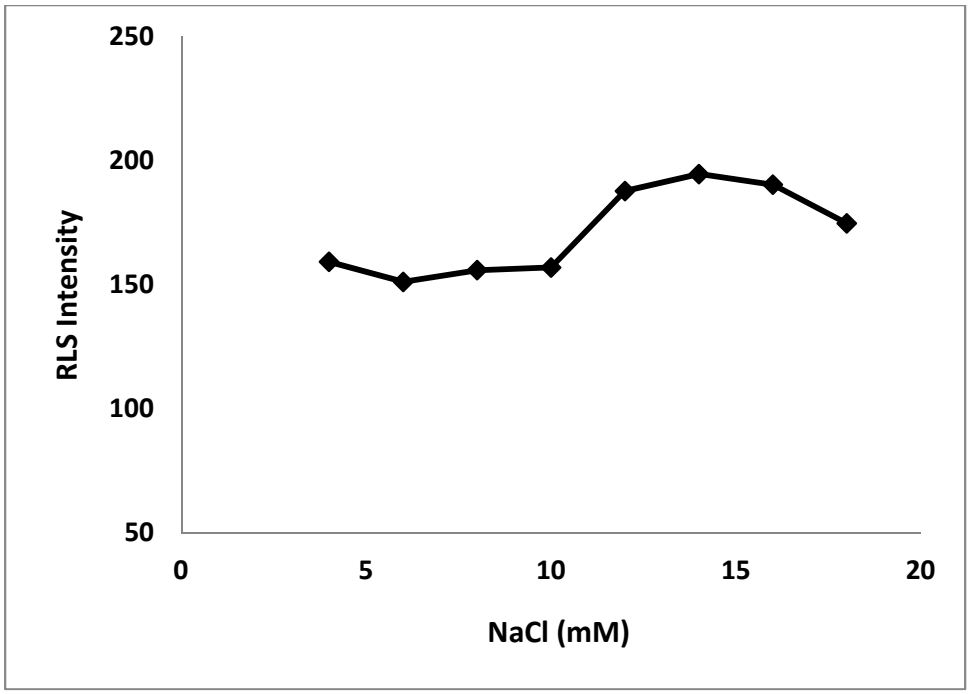

Fig. 3

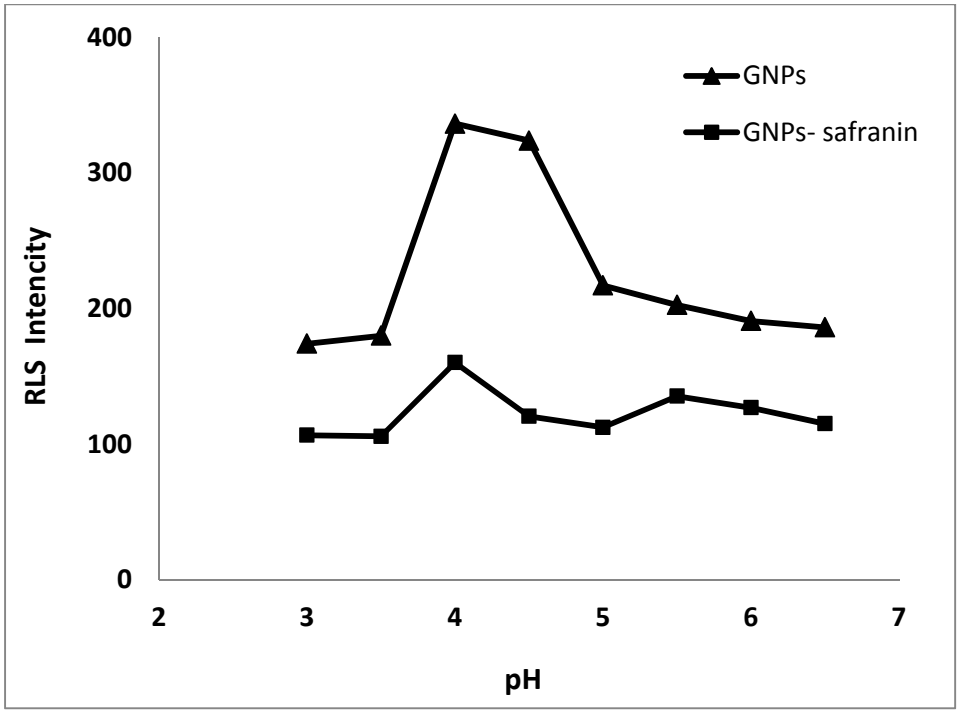

Fig. 4

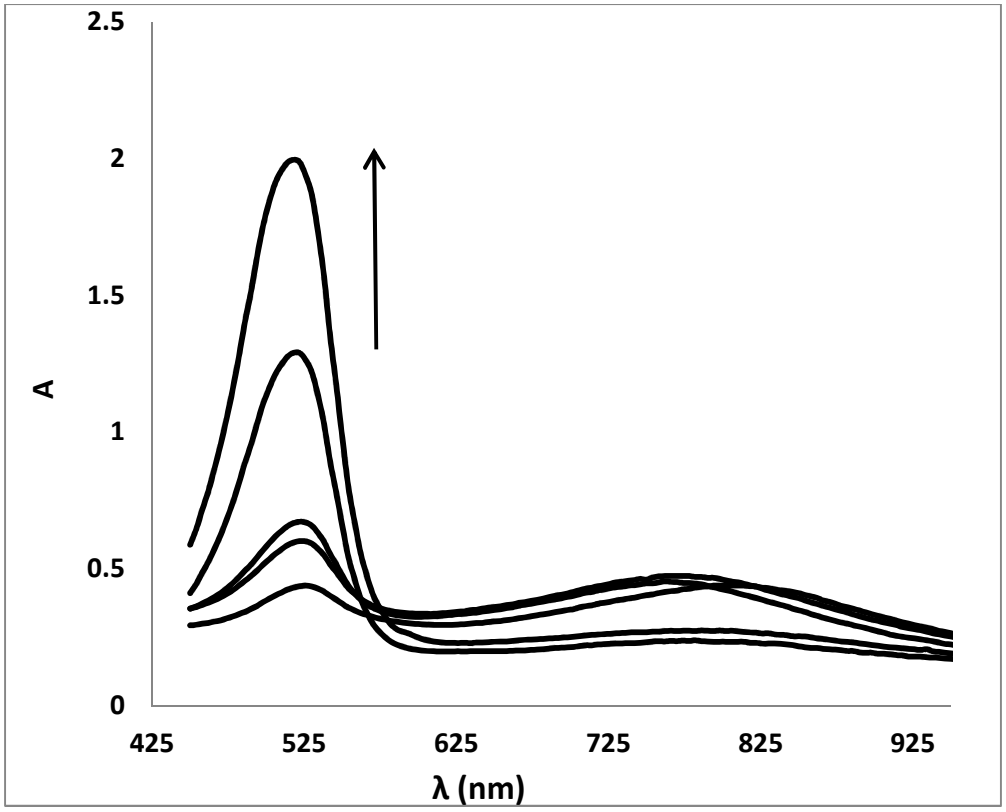

Fig. 5

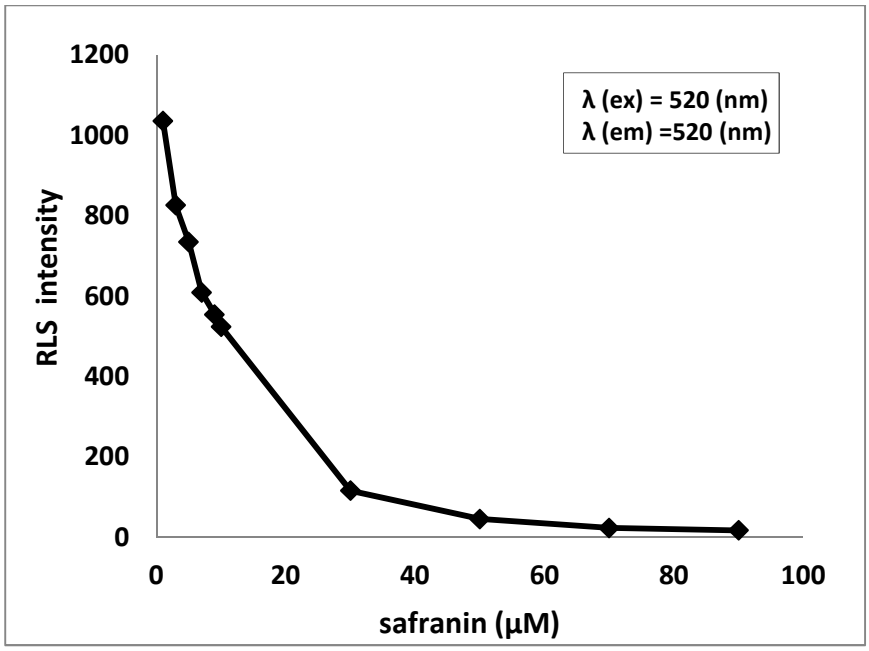

A: RLS spectrum of GNPs coated safranin

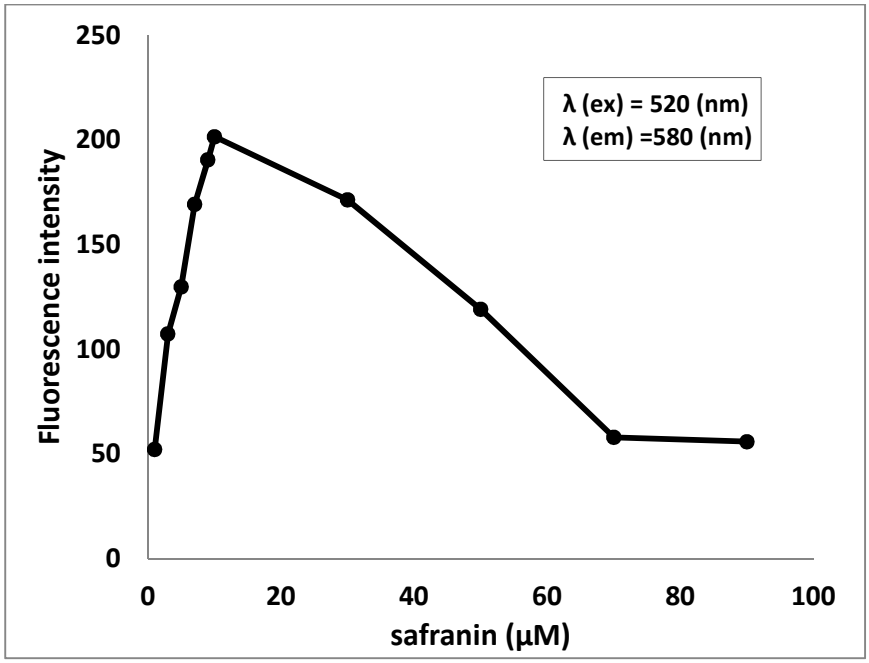

B: Fluorescence spectrum of safranin solution

Fig. 6

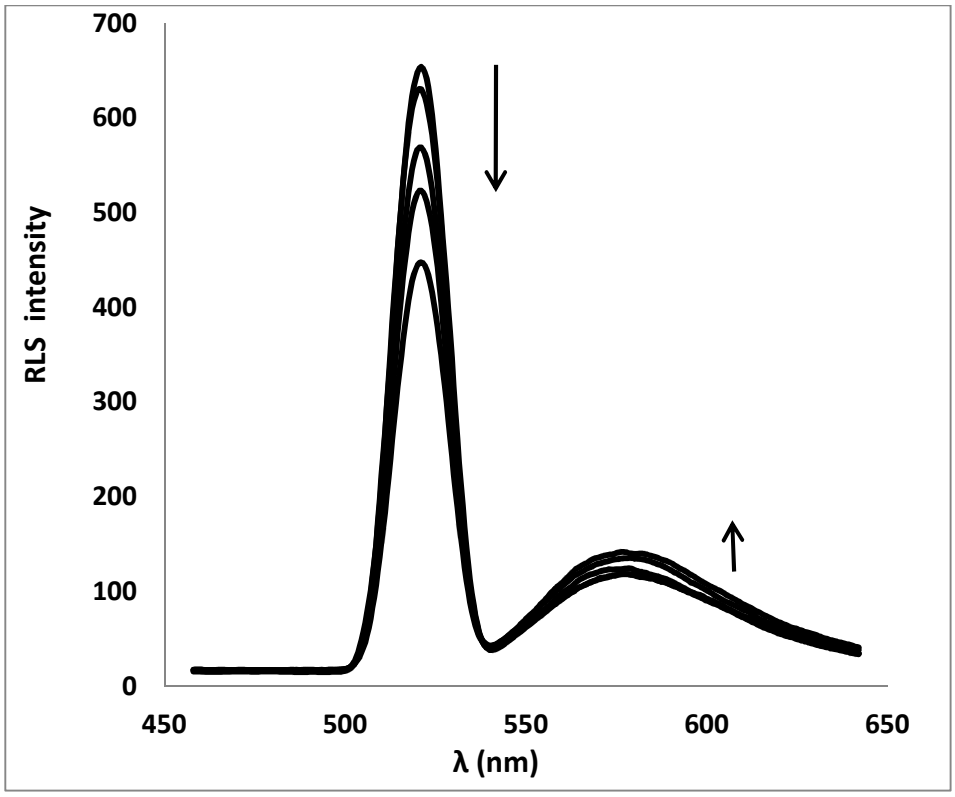

Fig. 7

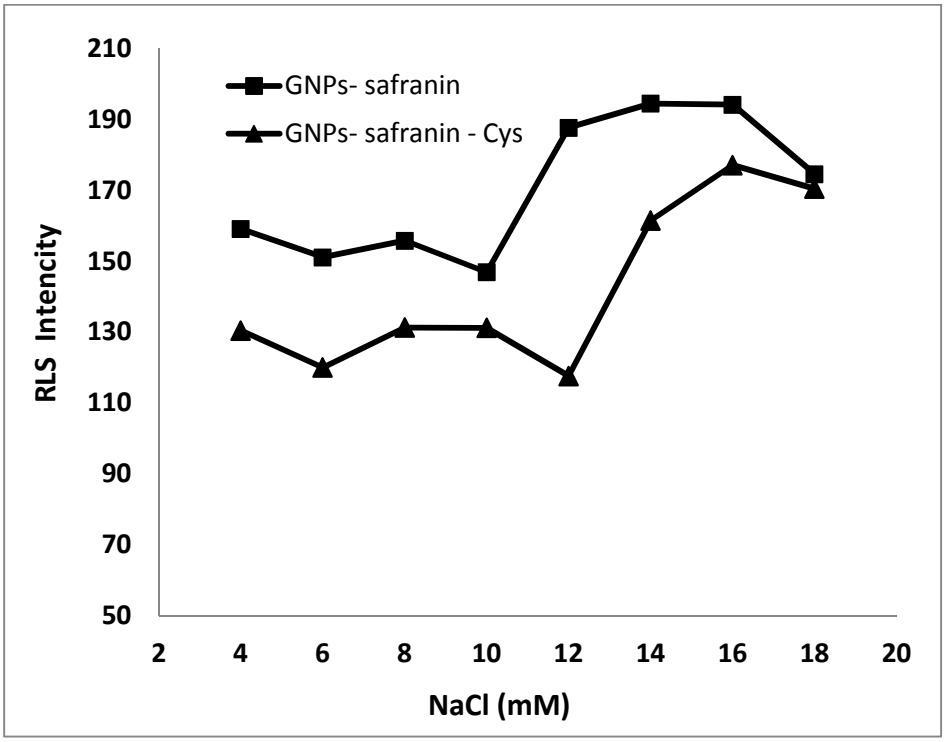

Fig. 8

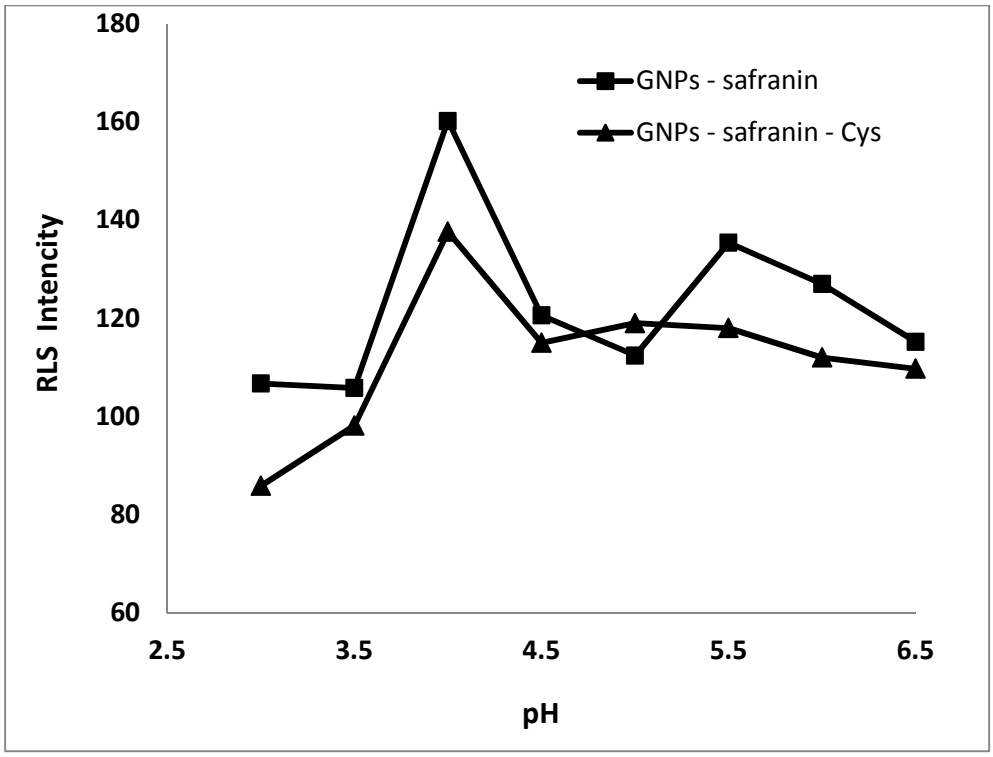

Fig. 9

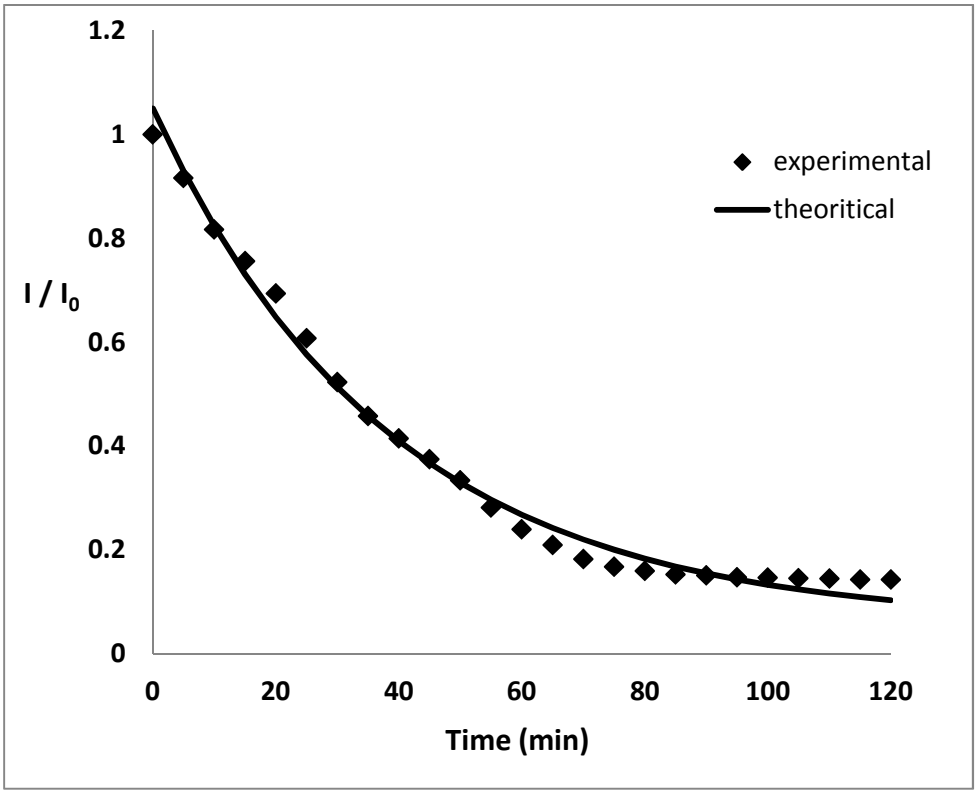

Fig. 10

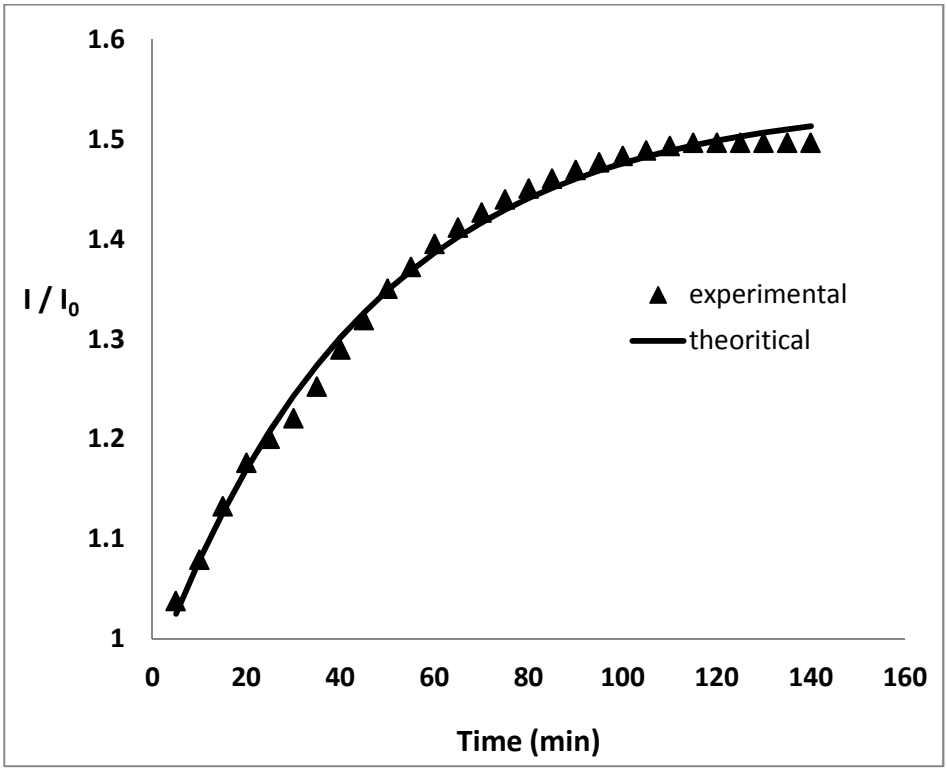

Fig. 11